A&A 469, 503–510 (2007)
DOI: 10.1051/0004-6361:20066477

Astronomy & Astrophysics

REM near-IR and optical multiband observations of PKS 2155-304 in 2005⋆

A. Dolcini[1], F. Farfanelli[2], S. Ciprini[2], A. Treves[1], S. Covino[3], G. Tosti[2], E. Pian[4], B. Sbarufatti[1], E. Molinari[3], G. Chincarini[3,5], F. M. Zerbi[3], G. Malaspina[3], P. Conconi[3], L. Nicastro[6], E. Palazzi[6], V. Testa[7], F. Vitali[7], L. A. Antonelli[7], J. Danziger[4], G. Tagliaferri[3], E. Meurs[8], S. Vergani[8], A. Fernandez-Soto[9], E. Distefano[10], G. Cutispoto[10], and F. D'Alessio[7]

[1] Università degli Studi dell'Insubria, Dipartimento di Fisica e Matematica, via Valleggio 11, 22100 Como, Italy
e-mail: alberto.dolcini@gmail.com
[2] Dipartimento di Fisica e Osservatorio Astronomico, Università di Perugia, via. A. Pascoli, 06123 Perugia, Italy
[3] INAF - Osservatorio Astronomico di Brera, via E. Bianchi 46, 23807 Merate (LC), Italy
[4] INAF - Osservatorio Astronomico di Trieste, via G. B. Tiepolo 11, 34143 Trieste, Italy
[5] Università degli Studi di Milano-Bicocca, Dipartimento di Fisica, Piazza delle Scienze, 3, 20126 Milan, Italy
[6] INAF/IASF Bologna, via Gobetti 101, 40129 Bologna, Italy
[7] INAF - Osservatorio Astronomico di Roma, via Frascati 33, 00040 Monteporzio Catone, Italy
[8] Dunsink Observatory, Castleknock, Dublin 15, Ireland
[9] Observatori Astronomic, Universitat de Valencia, Aptdo. Correos 22085, Valencia 46071, Spain
[10] INAF - Osservatorio Astrofisico di Catania, via S. Sofia 78, 95123 Catania, Italy

Received 29 September 2006 / Accepted 26 March 2007

ABSTRACT

Context. Spectral variability is the main tool for constraining emission models of BL Lac objects.
Aims. By means of systematic observations of the BL Lac prototype PKS 2155-304 in the infrared-optical band, we explore variability on scales of months, days, and hours.
Methods. We made our observations with the robotic 60 cm telescope REM located at La Silla, Chile, and *VRIJHK* filters were used.
Results. PKS 2155-304 was observed from May to December 2005. The wavelength interval explored, the total number of photometric points, and the short integration time render our photometry substantially superior to previous ones for this source. On the basis of the intensity and colour, we distinguish three different states of the source, each lasting months, which include all those described in the literature. In particular, we report the highest state ever detected in the *H* band. The source varied by a factor of 4 in this band, much more than in the *V* band (a factor ≈2). The source softened with increasing intensity, in contrast to the general pattern observed in the UV-X-ray bands. On five nights in November we had nearly continuous monitoring for 2–3 h. A variability episode on a time scale of $\tau \approx 24$ h is well-documented, and a much more rapid flare with $\tau = 1$–2 h, is also apparent, but is supported by relatively few points.
Conclusions. The overall spectral energy distribution of PKS 2155-304 is commonly described by a synchrotron-self-Compton model. The optical infrared emission is in excess of the expectation of the model in its original formulation. This can be explained by a variation in the frequency of the synchrotron peak, which is not unprecedented in BL Lacs.

Key words. galaxies: active – galaxies: BL Lacertae objects: individual: PKS 2155-304

1. Introduction

The prototype of high frequency peaked BL Lac objects, PKS 2155-304 ($z = 0.116$, Falomo et al. 1991) has been observed in the entire electromagnetic spectrum from radio to TeV gamma-rays. It has been the target of several multifrequency campaigns, the main goal of which was to study the variability of the spectral energy distribution (SED), in order to constrain emission models. In particular, we refer to the 1991 and 1994 campaigns involving IUE, ROSAT, ASCA, EUVE and ground-based telescopes (see Edelson et al. 1995; Urry et al. 1997, and references therein). There were noticeable differences in source behaviour between those two epochs. While in 1991 the multiwavelength variability was almost achromatic and the X-ray variation led that in the UV by a couple of hours, the variability in 1994 was more pronounced in X-rays than in UV-optical, which lagged by two days. The general pattern was of a hardening of the spectrum with increasing intensity.

More recently, Zhang et al. (2006b) studied a large set of data covering the period 2000–2005 obtained with the XMM-Newton satellite, which allowed a direct comparison of the X-ray and UV-optical bands, the latter deriving from the Optical Monitor onboard the satellite. The complexity of the variability pattern is confirmed. Some episodes of achromatic variation were detected, but a general tendency of increasing variability amplitude

⋆ Table A1 is only available in electronic form at the CDS via anonymous ftp to cdsarc.u-strasbg.fr (130.79.128.5) or via http://cdsweb.u-strasbg.fr/cgi-bin/qcat?J/A+A/469/503

Table 1. Outline of observations accomplished in 2005.

Period of observation	Nights of observation	Number of photometric points	Total exposure time
May	6	129	14 520 s
September	8	159	18 080 s
October	3	102	11 590 s
November	21	1581	173 540 s
December	6	64	7030 s

with increasing frequency, and spectral hardening with increasing intensity was found.

Optical photometry has been performed by several groups on several occasions (see e.g. Miller et al. 1983; Smith et al. 1992; Xie et al. 1996; Paltani et al. 1997; Pesce et al. 1997; Fan & Lin 2000; Tommasi et al. 2001, and references therein). All this material is rather fragmented, consisting of few hours of observations during a few nights. The difficulty of a systematic observing campaign covering many nights is partly overcome by the possibility of observing by using remotely guided or robotic telescopes.

The REM telescope, originally designed for prompt detection of gamma ray bursts (see Molinari et al. 2006), is particularly apt for photometric studies of BL Lacs (see also the previous results for PKS 0537-441 by Dolcini et al. 2005; and for 3C 454.3 by Fuhrmann et al. 2006) and, being located at La Silla (Chile), it is ideal for studying PKS 2155-304.

We report on an extensive and intensive photometric campaign performed in 2005 in the V, R, I, J, H, K bands. For the total number of photometric points, the time resolution (minutes), and spectral range, this campaign seems to supersede all the IR-optical photometric material presented thus far.

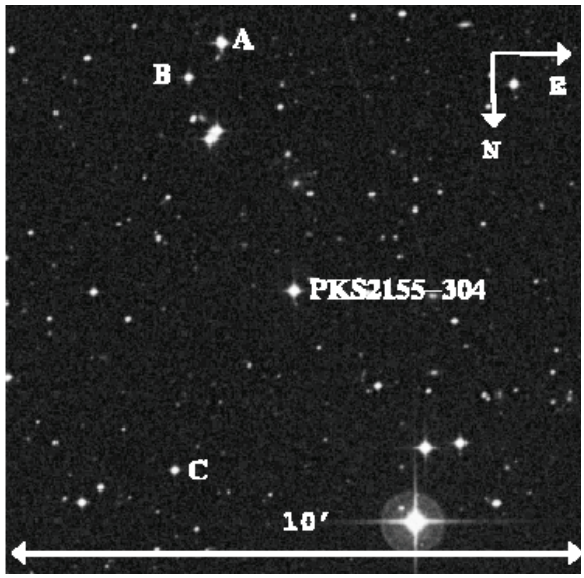

Fig. 1. PKS2155-304 field (DSS-1 survey). Letters indicate stars used for calibration.

2. REM, photometric procedure, data analysis

The Rapid Eye Mount (REM) Telescope is a 60 cm, fully robotic instrument. It has two cameras fed at the same time by a dichroic filter that allows the telescope to observe in the NIR (z', J, H, K), as well as optical (I, R, V). Further information on the REM project may be found in Zerbi et al. (2001), Chincarini et al. (2003), and Covino et al. (2004).

REM observed the PKS 2155-304 field during May, September, October, November, and December 2005 in *VRIH* bands. Only during three nights in September did the telescope also observe in J and K filters. To allow intranight and short time-scale variability monitoring, very intensive observations (2–3 h, quasi-continuously) were made during five of the nights in November. An outline of the observations is reported in Table 1, while the complete log is only available in electronic form at the CDS. Typical integration times are ≤100 s, and statistical uncertainties are always ≤10% and ≤3% in the highest state (November 2005, see below).

Reduction of the REM NIR and optical frames followed standard procedures. Photometric analysis of the frames was done using the GAIA[1] and DAOPHOT packages (Stetson 1986). Relative calibration was obtained by calculating magnitude shifts relative to three bright isolated stars in the field, indicated by A, B, C in Fig. 1 (image taken from ESO Digitized Sky Survey[2]).

The NIR frames were calibrated using the magnitudes of the A, B, and C stars as reported in the 2MASS catalogue[3]. For the optical, we exposed the standard field G156-31 (Landolt 1992) on 2006 June 29 and the PKS 2155-304 field immediately after this. We calculated the zero points that were then used to calibrate all of our data. The observed magnitudes in the REM filters for the reference objects A, B, and C are reported in Table 2. We monitored the relative intensities of the A, B, C reference stars during the entire observation period and have detected no variability within 0.1 mag (error on the average ≤0.01 mag).

Table 2. Coordinates, IR, and optical magnitudes for the reference stars.

	A	B	C
RA	21:58:46.505	21:58:43.807	21:58:42.337
Dec	–30:17:51.29	–30:17:15.71	–30:10:27.41
K	11.171 ± 0.024	12.475 ± 0.030	12.648 ± 0.024
H	11.182 ± 0.027	12.556 ± 0.026	12.769 ± 0.027
J	11.510 ± 0.027	12.838 ± 0.026	13.091 ± 0.029
I	12.184 ± 0.005	13.421 ± 0.009	13.216 ± 0.006
R	12.981 ± 0.004	13.434 ± 0.006	13.671 ± 0.010
V	13.179 ± 0.005	13.822 ± 0.009	13.899 ± 0.013

Note that we found significant deviations from the optical calibrations provided by the finding charts for AGN of Heidelberg University[4] (Hamuy & Maza 1989). In particular star C is also used as a calibrator by these authors, and our optical zeropoint differs by about 0.3 mag from theirs.

Relative and absolute calibration errors have been added in quadrature to the photometric error derived from the procedure.

[1] http://star-www.dur.ac.uk/~pdraper/gaia/gaia.html
[2] http://archive.eso.org/dss/dss
[3] http://irsa.ipac.caltech.edu
[4] http://www.lsw.uni-heidelberg.de/projects/extragalactic/charts/2155-304.html

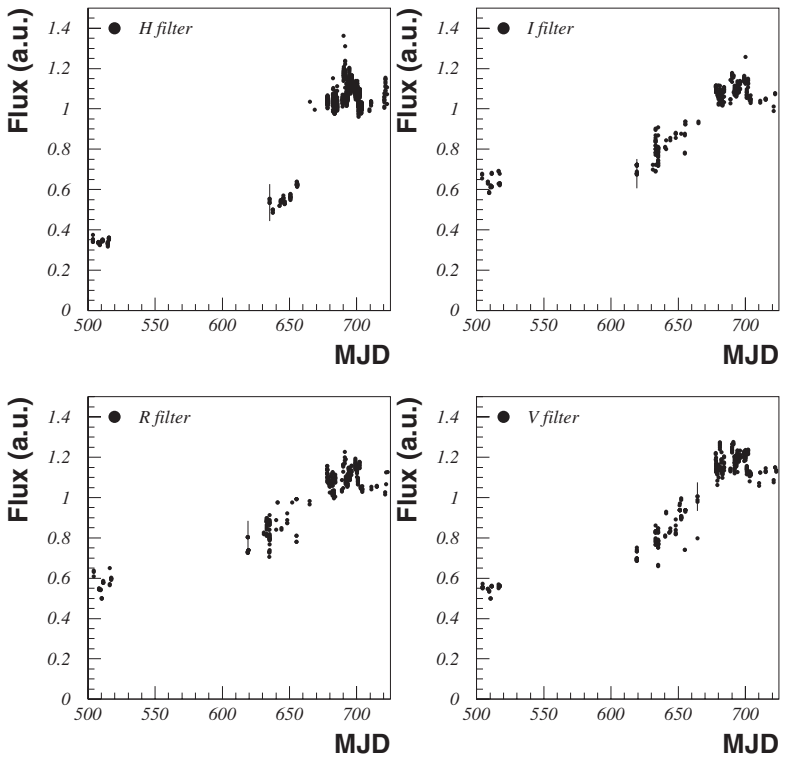

Fig. 2. Normalized light curves of PKS 2155-304. Flux is reported in arbitrary units (au). A typical error bar is plotted in each box.

Table 3. Average intensities for all epochs and all filters. All data are in mJy units.

Filter	*H*	*I*	*R*	*V*
Average	114.9 ± 23.3	38.4 ± 5.9	26.1 ± 5.8	20.8 ± 9.6
Max value	156.5	56.8	39.3	29.0
Min value	36.5	29.5	16.2	14.4
Average ep.1	39.3 ± 1.4	31.9 ± 1.5	18.7 ± 1.3	16.7 ± 0.7
Average ep.2	65.9 ± 5.2	35.7 ± 3.3	27.1 ± 3.2	20.4 ± 3.3
Average ep.3	122.9 ± 6.1	47.6 ± 2.9	32.3 ± 3.1	25.4 ± 3.1

3. Results

In this section we report the results of the long- and short-term variability study.

3.1. Long-term variability

The light curves in the *H*, *R*, *I*, *V* filters are given in Fig. 2. The intensity is normalized with respect to the average over the entire observation period. These averages are given in Table 3. It is immediately apparent that the total variability range is very different in the different filters, being a factor ≈4 in *H* and a factor ≈2 in *V* (see Table 3). The shapes of the light curves are similar in the various filters. A flare-like structure is apparent in all filters at $t \approx 680$ (first days of November). The ratio between the *V*- and *H*-band fluxes, designated as V/H, is reported in Fig. 3. In order not to introduce spurious effects due to small time-scale variability, the V/H ratio was computed for pairs of *V* and *H* measurements spaced apart in time by no more than 10 min.

It seems that there are two main colour states, meaning that the source softens rather abruptly, in response to the November flare. On the basis of the light curve and the colour curve, we divided the observations into three epochs: 1) 500–525 (May 2005), 2) 640–660 (September–October 2005), 3) 670–725 (November–December 2005), expressed in MJD[5].

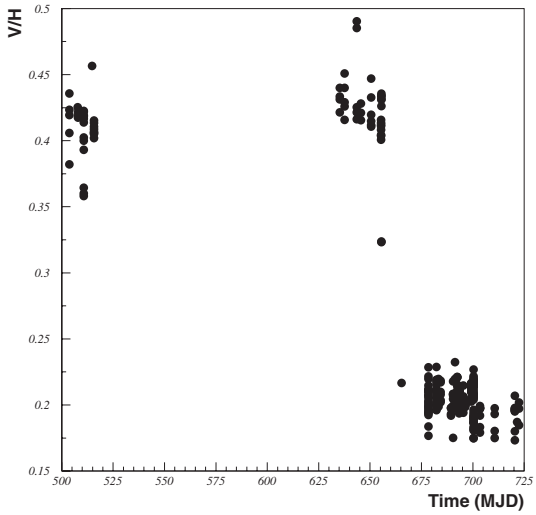

Fig. 3. V/H flux ratio evolution during 2005. Error bars are comparable to the symbol size.

3.2. Short time-scale variability

We report in Fig. 4 the light curves for five nights in November 2005, when the observations were more intensive. All the nights belong to epoch 3, corresponding to the high state of the source. The mean intensity and the 1-sigma values for each night are given in Table 4.

[5] For the modified Julian date we use the convention MJD = JD-2 453 000.5.

Table 4. Average intensities and 1-sigma values for all filters for all five nights with more intensive observations in November 2005 (all values in mJy units).

Night	4/11	8/11	18/11	19/11	20/11
Average H	119.3 ± 1.7	119.3 ± 3.0	120.4 ± 2.1	124.5 ± 2.8	130.8 ± 3.0
Average I	49.7 ± 0.6	47.0 ± 0.5	49.3 ± 0.6	49.3 ± 0.6	49.0 ± 0.7
Average R	34.9 ± 0.8	32.8 ± 1.3	33.7 ± 0.5	34.4 ± 1.6	33.5 ± 0.5
Average V	24.8 ± 1.1	24.6 ± 1.1	25.0 ± 1.1	25.1 ± 1.1	26.3 ± 0.1

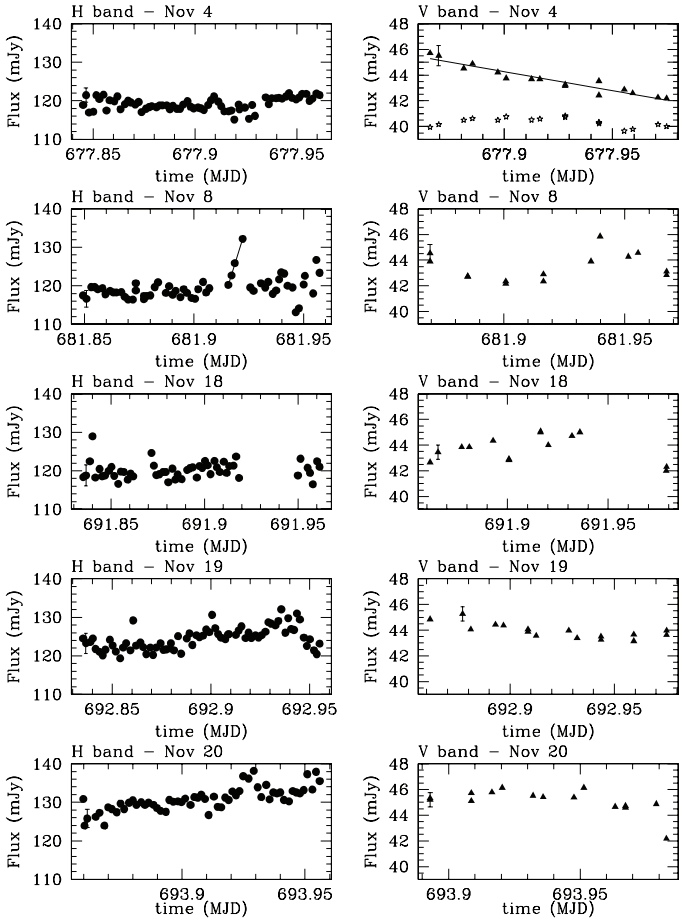

Fig. 4. Light curves in the H and V filters for five nights in November 2005, when the observations were more intensive. Dates of observations are reported in each box. The solid line in the V band – 4 Nov. box results from a linear regression analysis. The solid line in the H band – 8 Nov. box connects the four points of the flare-like structure. In each box a typical error bar is given. In V band – 4 Nov. box, the light curve of one comparison star is also plotted, with a fixed enhancement of 14 mJy.

A χ^2 analysis indicates that in each night the significance of variability is very high, except for the nights of November 4 and November 18 for the H band and November 19 for the V band. In the box of Nov. 4 – V band we also report the photometry of a comparison star that illustrates the significance of the source variability directly. Though the shapes of intensity curves are different (see Fig. 4), there is a rather regular colour-intensity dependence (see Fig. 5) indicating harder states for higher intensities.

We adopted the usual definition of time-scale variability $\tau = \frac{1}{1+z}\frac{\langle f\rangle}{\mathrm{d}f/\mathrm{d}t}$. Following Montagni et al. (2006), a variability time scale was taken as reliable if the light curve can be approximated with a linear dependence, and it contains at least 10 points. In particular, this gives a time scale of ≈24 h for the November 4 night (Fig. 4, V band – Nov. 4 box). The simultaneous H light curve does not show any regular variability. We note that on November 8 there is a flare-like event in the H curve. If one connects 4 points as suggested in the Fig. 4 H band – Nov. 8 box, the time scale variability is as short as 1.5 h. Unfortunately the V light curve is too sparse to also confirm the presence of the flare in this band.

3.3. The NIR-optical spectral energy distribution

We had a six-filter coverage (K, H, J, I, R, V) during three nights of September 2005 (epoch 2) and representative SEDs for these nights are reported in Fig. 6.

The delays between exposures in the different filters are less than 20 min. Reddening corrections are less than 6% in V so have been neglected. A fit with a single power law yields $\alpha \approx 0.9$, which is clearly not good. The main deviation derives from the J filter, substantially exceeding our photometric precision of about 10%. An improvement in the fit was obtained by using a broken power law with spectral indices $\alpha \approx 0.4$ for the IR data and $\alpha \approx 0.9$ for the optical data. For comparison, we report in Fig. 7 the SED of the 2006 June 29 exposure used for calibration purposes: its profile is rather similar to that of September 2005. At the other epochs the SED consist of 4 points (H, I, R, V), and in Figs. 8 and 10 we give representative examples of SEDs acquired on epochs 1 and 3. The time differences between observations at various filters are less than 20 min.

In Fig. 8, which refers to a low state, we also report the estimated contribution from the host galaxy, which was calculated by adopting both the H magnitude of the galaxy measured by Kotilainen et al. (1998) and the Mannucci et al. (2001) template spectrum for giant ellipticals. It is apparent that the contribution of the galaxy never exceeds 20% of the BL Lac signal. At the other epochs, the contribution from the galaxy is negligible, so it is not relevant for explaining the excess in J with respect to the single power law noted above. The epoch 2 photometry (Fig. 9) is compared with spectrophotometry obtained with the ESO 3.6 m telescope by R. Falomo[6] on July 25, 2001 (Sbarufatti et al. 2006). The source was found in a similar, but somewhat lower brightness state and some deviations from a power law are apparent. The *HRIV* points at epoch 3 (Fig. 10) are well-fitted by a single power law of $\alpha \approx 1.3$. The goodness of the fit may be partly misleading, because as discussed above, the six filter fits of epoch 2 with a single power law are not satisfactory. In any case the comparison of the SEDs at the three epochs clearly indicates a softening with increasing intensity.

4. Discussion

A collection of near-IR/optical SEDs of PKS 2155-304 obtained by various authors at different epochs is presented in Fig. 11

[6] spectrum available at the ZBLLAC online library, `http://www.oapd.inaf.it/zbllac`

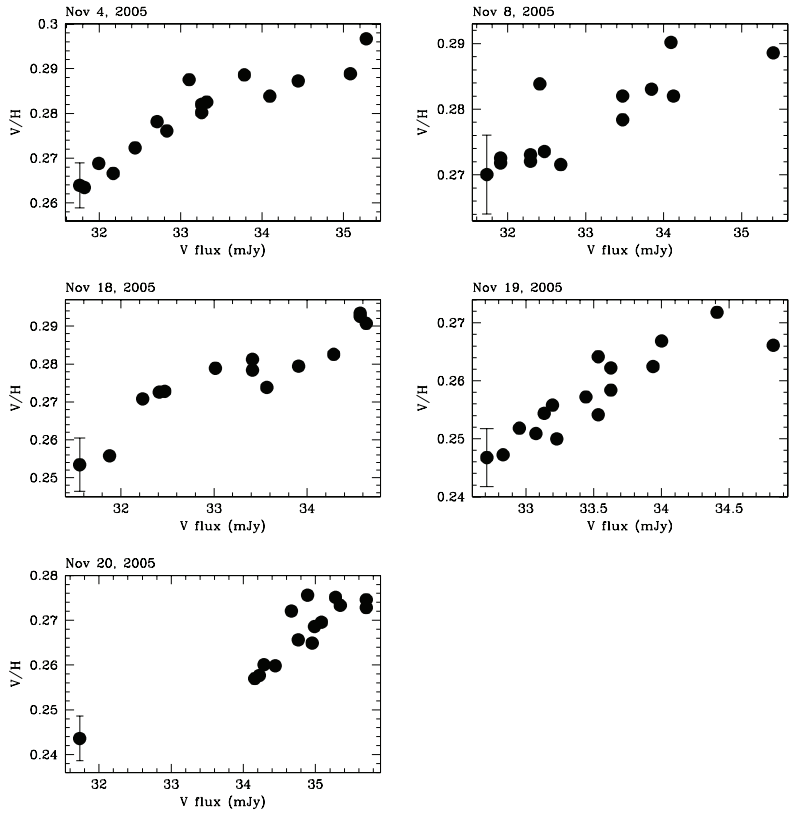

Fig. 5. V/H flux ratio versus intensity for the five more intensively observed nights of epoch 3. A typical error bar is plotted in each box.

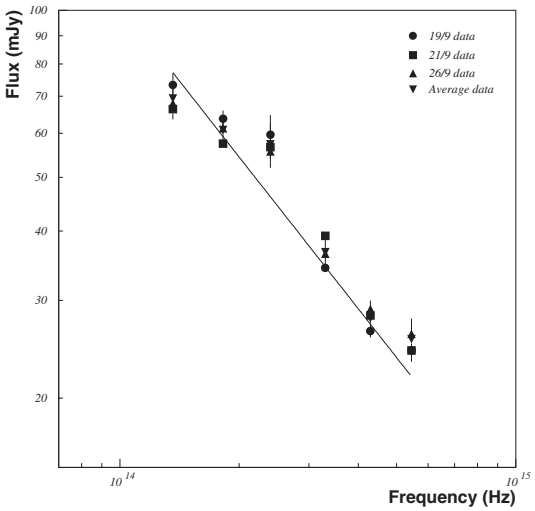

Fig. 6. September 2005 spectra for observations including the K and J filters. The spectral fit on average data with a single power law yields a spectral index $\alpha = 0.91 \pm 0.07$.

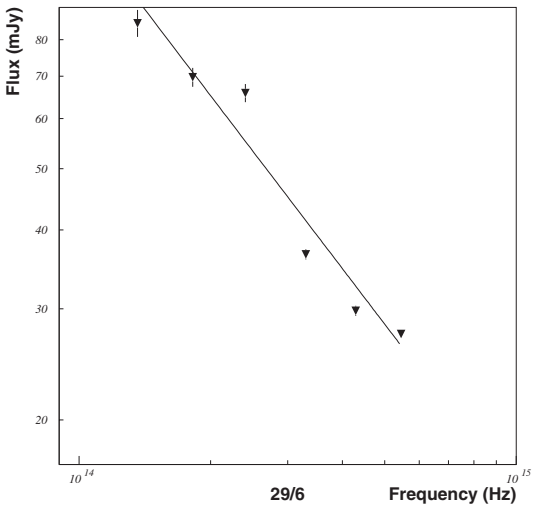

Fig. 7. 2006 June 29 spectrum. The spectral fit with a single power law yields a spectral index of $\alpha = 0.90 \pm 0.16$.

and in Table 5. Our data encompass all those reported in the literature.

In the historical observations of PKS 2155-304, the delays between exposures at different filters are typically of the order of hours, instead of about 10 min as in our data set. Comparing literature data with our data, it is apparent that the maximum we observed on November 20, 2005 in the H filter light curve is the highest state ever reported in this band. Note that the V state was comparable to the states reported in the literature, very likely because the coverage of the source in the optical band is less sparse than in the NIR. A very noticeable result of our photometry is the discovery of long-term H-band variability, the amplitude of which is much greater than in the optical.

In Fig. 12 we plot the spectral index vs. the V magnitude, as reported in Table 5. There is no apparent correlation. It is noticeable, however, that the highest state in all bands (our observation of November 2005) corresponds to a rather soft spectral shape. This contrasts with the source's usual behaviour of hardening with increasing intensity, as found in the UV-X-ray band (see Introduction). It contrasts also with the short time scale variability, as reported in Sect. 3.2.

There is a general consensus that the blazar SED can be explained by the superposition of a synchrotron component and

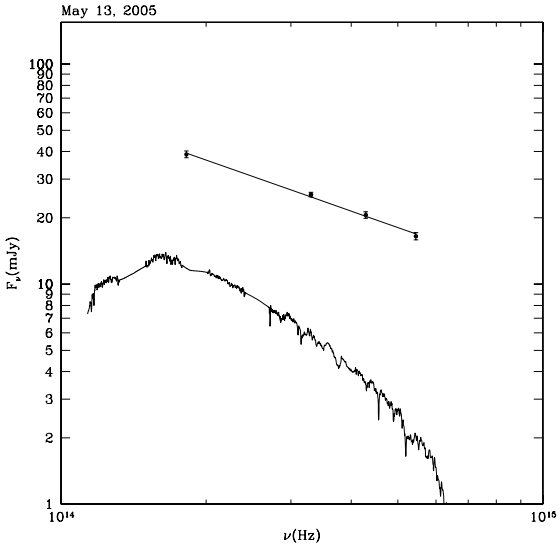

Fig. 8. 2005 May 13 spectrum – epoch 1. We also report the spectrum of the host galaxy (see text). The spectral fit with a single power law yields a spectral index of $\alpha = 0.77 \pm 0.16$.

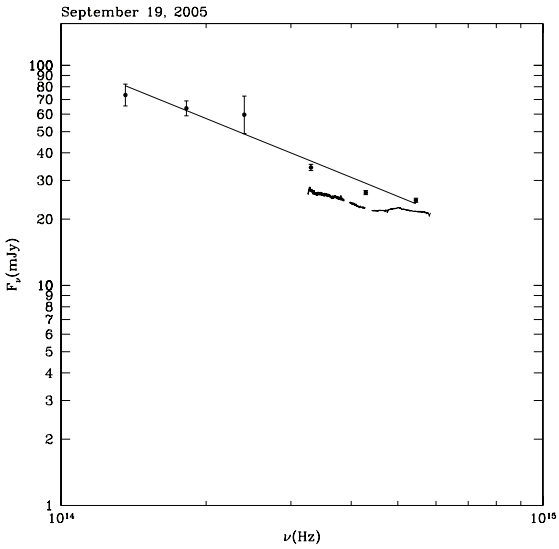

Fig. 9. 2005 September 19 spectrum – epoch 2. For comparison we report the ESO 3.6 m telescope spectrophotometry that corresponds to a slightly lower state of the source. The spectral fit with a single power law yields a spectral index of $\alpha = 0.88 \pm 0.05$.

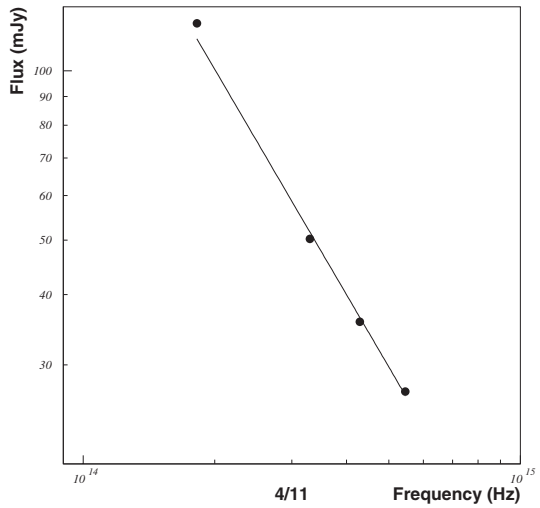

Fig. 10. 2005 November 4 spectrum – epoch 3. The spectral fit with a single power law yields a spectral index $\alpha = 1.33 \pm 0.10$. Error bars are comparable with symbol size.

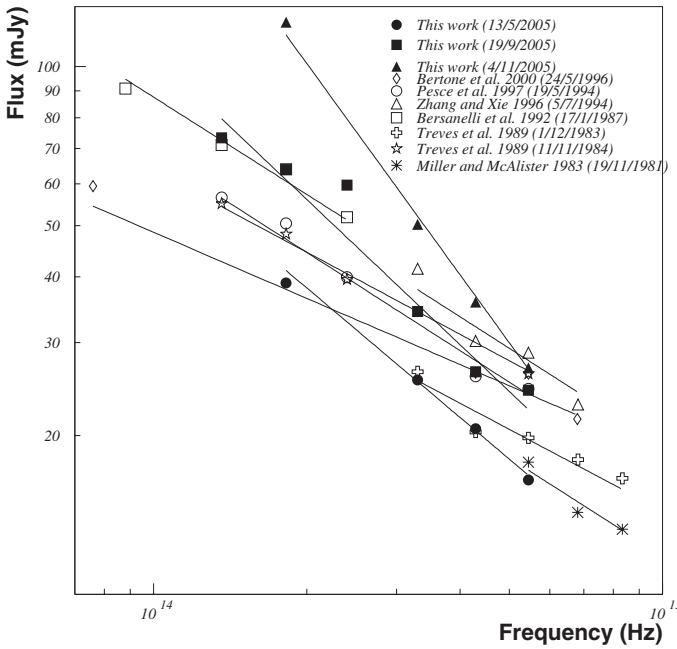

Fig. 11. Different spectra of PKS 2155-304 from observations at other epochs reported in the literature. Symbols correspond to the following works: filled circles, this work (13/5/2005 data); filled squares, this work (19/9/2005 data); filled triangles, this work (4/11/2005 data); open diamonds, Bertone et al. (2000; 24/5/1996 data); open circles Pesce et al. (1997; 19/5/1994 data, the Hamuy & Maza (1989) calibration is used); open up triangles, Zhang & Xie (1996; 5/7/1994 data); open squares, Bersanelli et al. (1992; 17/1/1987 data); open crosses, Treves et al. (1989; 1/12/1983 data); open stars, Treves et al. (1989; 11/11/1984 data); asterisks, Miller & McAlister (1983; 19/11/1981 data). Spectral index values and V magnitudes for all data sets are reported in Table 5.

an inverse Compton one due either to scattering off the synchrotron photons (synchrotron-self Compton, SSC) or to external photons like those of the broad line region or of a thermal disk (e.g. Tavecchio et al. 1998; Katarzynski et al. 2005). This results in a typical two-maxima shape of the blazar SED. In Fig. 13 we report examples of the SED modeling proposed for PKS 2155-304 on the basis of data taken in 1997. The models are explained in Chiappetti et al. (1999). The object is a typical HBL, with the synchrotron peak in the soft X-rays.

A well-known critical point of this model is that the source size is essentially constrained by variability, and variability itself requires that the SED is constructed using simultaneous observations in all bands. A further step of the modelling consists in identifying the physical origin of the relativistic jet and of its variability; see e.g. Katarzynski & Ghisellini (2007). With this premise it is obvious that the optical-IR photometric study, non simultaneous with that in other regions of the SED, only has a limited relevance in clarifying the overall picture.

However, we would like to make some remarks. If the SSC models reported in Fig. 13 truly represent the behaviour of the SED in 1997, as suggested by the good match with the X-ray and TeV energy data, and if our 2005 optical-IR spectra are also due to the SSC mechanism, then the latter represent a different condition in the jet and point to different critical

Table 5. Spectral index values and V values for all spectra plotted in Fig. 11.

Data set	α	V (mJy)
This work (13/5/2005)	0.77 ± 0.16	16.485 ± 0.263
This work (19/9/2005)	0.88 ± 0.05	24.370 ± 0.238
This work (4/11/2005)	1.33 ± 0.10	26.884 ± 0.489
Bertone et al. (2000)	0.42 ± 0.26	26.20 ± 0.58
Pesce et al. (1997)	0.62 ± 0.30	24.50 ± 0.67
Zhang & Xie (1996)	0.62 ± 0.16	22.90 ± 0.63
Bersanelli et al. (1992)	0.61 ± 0.38	51.88 ± 1.56 (J band)
Treves et al. (1989) (1/12/1983)	0.51 ± 0.31	19.80 ± 0.36
Treves et al. (1989) (11/11/1984)	0.51 ± 0.41	26.20 ± 0.48
Miller & McAlister (1983)	0.62 ± 0.56	17.8

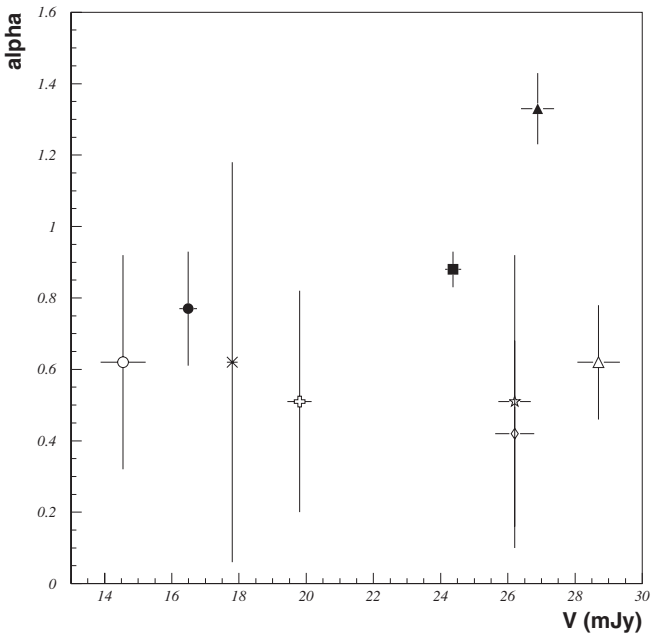

Fig. 12. α vs. V plot for data reported in Fig. 11. Symbols are the same as in Fig. 11.

parameters within the SSC scenario. While the IR-optical spectrum in May 2005 has the same shape as predicted in 1997, but different normalization, the 2005 November IR-optical spectrum is different in both shape and normalization. The 2005 May observation suggests that the synchrotron peak may be located at a frequency similar to the one observed in 1997 (approximately between extreme UV and soft X-rays), the total energy being somewhat higher (about a factor 2, see Fig. 13) than observed in 1997. The slope of the 2005 November spectrum instaed suggests a much lower synchrotron peak energy, around the IR-optical domain or even redward, i.e. about 2–3 orders of magnitude lower than observed in 1997 and inferred in May 2005. While a variation in the synchrotron peak energy of this amplitude and on this time scale (the 2005 September slope is intermediate between those of May and November 2005, suggesting a monotonic change), it is not unprecedented in blazars (Mkn501 exhibited a similar variation on a much more rapid time scale, Pian et al. 1998). This would be the first observation of this kind in PKS 2155-304. Therefore, our interpretation is only tentative, although supported by the large observed IR variability.

Alternatively, in order to explain the optical-IR flux excess we observed in 2005 with respect to the SSC prediction based on the earlier multiwavelength data (Fig. 13), one could invoke a thermal component, possibly from hot dust associated

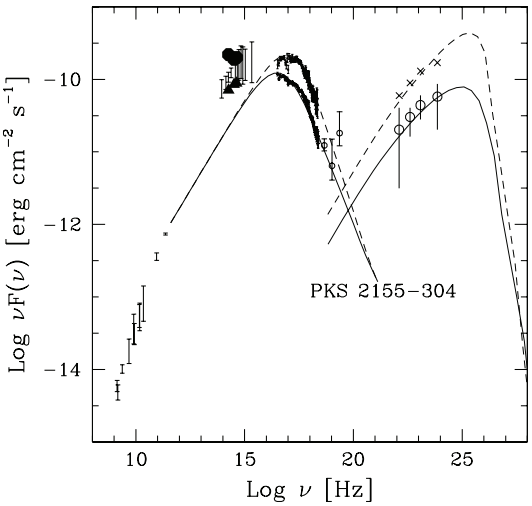

Fig. 13. SED of PKS 2155-304 in two states, adapted from Chiappetti et al. (1999) (see text for details). Data from this work are also plotted. Filled triangles correspond to epoch 1 (13/5/2005 data), while filled hexagons belong to epoch 3 data (20/11/2005). Optical, UV and REM data are dereddened using $E(B-V) = 0.026$ and parameters given by Cardelli et al. (1989).

with the "dusty torus" surrounding the central region of the active nucleus, as suggested in the cases of other blazars with excess in the optical-infrared band (De Diego et al. 1997, for blazar 3C 66A; Pian et al. 1999 for 3C 279; Pian et al. 2002, 2007, for blazar PKS 0537-441). However, this seems somewhat less likely, because high emission states, as observed by us, are expected to be dominated by non-thermal beamed relativistic radiation.

The continuation of this and other similar optical-IR studies, which have been proven to be promising but do not provide enough information for a physical interpretation of the data, requires that the observations are extended to other wavelengths. Simultaneous observations over a wide wavelength range is the only tool that provides the necessary information for physically interpretating of the observed variability of blazars. REM monitorings of the kind reported here could be an effective trigger for X-ray satellites, and programmes along these lines are foreseen with SWIFT. Cross-correlation procedures, which up to now have mainly been limited to the X-ray band (Zhang et al. 2005, 2006a,b; Sembay et al. 2002; Edelson et al. 1995) should be extended to a much larger portion of the SED.

References

Bersanelli, M., Bouchet, P., Falomo, R., & Tanzi, E. G. 1992, AJ, 104, 28
Bertone, E., Tagliaferri, G., Ghisellini, G., et al. 2000, A&A, 356, 1
Cardelli, J. A., Clayton, G. C., & Mathis, J. S. 1989, ApJ, 345, 245
Chincarini, G., Zerbi, F., Antonelli, A., et al. 2003, The Messenger, 113, 40
Covino, S., Stefanon, M., Fernandez-Soto, A., et al. 2004, SPIE, 5492, 1613
Chiappetti, L., Maraschi, L., Tavecchio, F., et al. 1999, ApJ, 521, 552
De Diego, J. A., Kidger, M. R., Gonzáles-Pérez, J. N., & Letho, H. J. 1997, A&A, 318, 331
Dolcini, A., Covino, S., Treves, A., et al. 2005, A&A, 443, L33
Edelson, R., Krolik, J., Madejski, G., et al. 1995, ApJ, 438, 120
Falomo, R., Giraud, E., Maraschi, L., et al. 1991, ApJ, 380, L67
Falomo, R., Bersanelli, M., Bouchet, P., & Tanzi, E. M. 1993, AJ, 106, 11
Fan, J. H., & Lin, R. G. 2000, A&A, 355, 880
Fuhrmann, L., Cucchiara, A., Marchili, N., et al. 2006, A&A, 445L, 1
Hamuy, M., & Maza, J. 1989, AJ, 97, 720

Katarzynski, K., & Ghisellini, G. 2007, A&A, 463, 529
Katarzynski, K., Ghisellini, G., Tavecchio, F., et al. 2005, A&A, 433, 479
Katarzynsky, K., Ghisellini, G., Mastichiadis, A., et al. 2006, A&A, 453, 47
Kotilainen, J. K., Falomo, R., & Scarpa, R. 1998, A&A, 336, 479
Landolt, A. U. 1992, AJ, 104, 340
Mannucci, F., Basile, F., Poggianti, B. M., et al. 2001, MNRAS, 326, 745
Miller, H. R., & McAlister, H. A. 1983, ApJ, 272, 26
Molinari, E. Vergani, S. D., Malesani, D., et al. 2006 [arXiv:astro-ph/0612607]
Montagni, F., Maselli, A., Massaro, E., et al. 2006, A&A, 451, 435
Paltani, S., Courvoisier, T. J.-L., Blecha, A., & Bratschi, P. 1997, A&A, 327, 539
Pesce, J. E., Urry, C. M., Maraschi, L., et al. 1997, ApJ, 486, 770
Pian, E., Vacanti, G., Tagliaferri, G., et al. 1998, ApJ, 492, L17
Pian, E., Urry, C. M., Maraschi, L., et al. 1999, ApJ, 521, 112
Pian, E., Falomo, R., Hartman, R. C., et al. 2002, ApJ, 392, 407
Pian, E., Romano, P., Treves, A., et al. 2007, ApJ, in press [arXiv:astro-ph/0704.0958]
Sbarufatti, B., Falomo, R., Treves, A., & Kotilainen, J. 2006, A&A, 457, 35
Sembay, S., Edelson, R., Markowitz, A., et al. 2002, ApJ, 574, 634
Smith, P. S., Hall, P. B., Allen, R. G., & Sitko, M. L. 1992, ApJ, 400, 115
Stetson, P. B. 1986, PASP, 99, 191
Tavecchio, F., Maraschi, L., & Ghisellini, G. 1998, ApJ, 509, 608
Tanihata, C., Kataoka, J., Takahashi, T., & Madejski, G. M. 2004, ApJ, 601, 759
Tommasi, L., Diaz, R., Palazzi, E., et al. 2001, ApJS, 132, 73
Treves, A., Morini, M., Chiappetti, L., et al. 1989, ApJ, 341, 733
Urry, C. M., Maraschi, L., Edelson, R., et al. 1997, ApJ, 486, 799
Xie, G. Z., Zhang, Y. H., Li, K. H., et al. 1996, AJ, 111, 3
Zerbi, F. M., Chincarini, G., Ghisellini, G., et al. 2001, AN, 322, 275
Zhang, Y. H., & Xie, G. Z. 1996, A&AS, 116, 289
Zhang, Y. H., Treves, A., Celotti, A., Qin, Y. P., & Bai, J. M. 2005, ApJ, 629, 686
Zhang, Y. H., Treves, A., Maraschi, L., Bai, J. M., & Liu, F. K. 2006a, ApJ, 637, 699
Zhang, Y. H., Bai, J. M., Zhang, S. N., et al. 2006b, ApJ, 651, 682